NG-IVIM treatment response prediction

Investigating DWI Biomarkers for Personalizing Treatment in HPV-negative Oropharyngeal Squamous Cell Carcinoma

T.S. du Pon

Delft University of Technology

TU Delft

Erasmus MC Cancer Institute

NG-IVIM treatment response prediction

Investigating DWI Biomarkers for Personalizing Treatment in HPV-negative Oropharyngeal Squamous Cell Carcinoma

by

T.S. du Pon

in partial fulfilment of the requirements of

Master of Science

Biomedical Engineering

Track medical physics

at the Delft University of Technology,

to be defended publicly on Friday August 23, 2024 at 03:45 PM.

Student number:	4933877	
Project duration:	March 1, 2024 – August 23, 2024	
Thesis Supervisors:	Prof. dr. J.A. Hernandez-Tamames,	TU Delft
	dr. ir. S.F. Petit,	Erasmus MC
	ir. I. Lauwers,	Erasmus MC
Thesis committee:	Prof. dr. J.A. Hernandez-Tamames,	TU Delft(chair)
	dr. ir. D. H. J. Poot,	Erasmus MC
	ir. I. Lauwers,	Erasmus MC

This thesis is confidential and cannot be made public until August 19, 2026.

TU Delft

Erasmus MC Cancer Institute

Acknowledgements

The work on this thesis has been carried out as part of the Erasmus MC's Department of Radiotherapy. The author would like to thank several people for their contributions to this thesis project. First of all, a special thanks to ir. Iris Lauwers and dr. ir. Steven Petit for their daily supervision. Furthermore, thanks to drs. Gerda Verduijn for adjusting the GTVs and for her feedback during weekly meetings. Also thanks to dr. Marta Capala for her feedback during the weekly meetings. Moreover, a special thanks to prof. dr. Juan Hernandez-Tamames for chairing the defense and supervision during the project, and dr. ir. Dirk Poot for participating in the thesis committee.

Additionally, I would like to thank Martine van der Knaap for helping out with completion of the scan database, and to dr. András Zolnay for helping out with the use of Uluru and Matterhorn. Finally, thanks to the Erasmus MC outcome unit for gathering treatment outcomes.

T.S. du Pon
Delft, August 2024

Abstract

Background: Oropharyngeal squamous cell carcinoma (OPSCC) not associated with the human papillomavirus (HPV) have a poor prognosis compared to their HPV-associated counterpart. In literature diffusion-weighted imaging (DWI) shows great potential as a biomarker for treatment response in HPV-associates OPSCC. For this study the possibility of using DWI parameters as biomarker for treatment response during treatment of HPV-negative OPSCC is investigated. Tumor size and shrinkage have also been investigated.

Methods: In this study sixteen patients with HPV-negative OPSCC who underwent (chemo-)radiotherapy have been included. All are current and/or former smokers. At two time point an DWI-MRI scan took place, before and 2 weeks into treatment. The mean apparent diffusion coefficient (ADC) and Non-Gaussian Intravoxel Incoherent Motion Imaging (NG-IVIM) parameters based on the gross tumor volume (GTV) have been calculated. The parameters and differences in parameters have been compared between patients that responded well to treatment and patients with progressive disease.

Results: At pre- and midtreatment no significant differences have been found between the Complete Response (CR) and Progressive Disease(PD) patient groups. Diffusion coefficient D showed a significant change between pre- and midtreatment, with an increase for PD and decrease for CR. When comparing the residual region to the region that had disappeared after two weeks based on pretreatment data significant differences have been found in ADC, D and f for CR, as well as f for PD.

Conclusion Changes in D during treatment have shown to be a significant predictor for treatment response. However this study is limited by a small patient group and more research with larger cohorts and additional biomarkers is needed to develop reliable clinical decision-making tools.

Contents

1. Introduction

Oropharyngeal cancer is among the six most common cancertypes in the world, with at least 90% of cases being squamous cell carcinomas (SCC) [2]. The five year survival rate of Oropharyngeal squamous cell carcinomas (OPSCC) patients is below 50% [3, 4]. Historically, tobacco and alcohol were believed to be the main causes of OPSCC. However, a 2001 study by Mork et al. [5] identified a link between OPSCC and human papillomavirus (HPV).

Although patients with OPSCC not related to HPV are fewer than those with HPV-associated OPSCC [6], they still represent an important group for research. Patients without HPV-associated OPSCC have a poorer prognosis than those with HPV-associated OPSCC. [7, 8, 9, 10, 11, 12, 13, 14]. The American Joint Committee on Cancer and the Union for International Cancer Control eight-edition TNM staging guideline (TNM8) even classify OPSCC based on HPV differently [15]. In addition to the poor prognosis, radiotherapy in the neck region often causes a variety of side effects, such as skin irritations and dry mouth due to reduced salivary gland productivity [16]. The lower quality of life due to side effects combined with the poor prognosis raises the question of whether treatment is worth it for all patients.

The HolistiC early respOnse assessMent for oroPharyngeaL cancEr paTiEnts trial (COMPLETE) is a single-centre trial by the Erasmus MC, the general objective of this study is to investigate biomarkers to predict response to treatment in patients with HPV-negative OPSCC, as described by Verduijn et al. in [17]. By predicting the response, it is possible to personalize treatment for patients who have a high change of treatment failure. In the COMPLETE trial non-gaussian Intravoxel Incoherent Motion (NG-IVIM) magnetic resonance imaging (MRI) is one of these biomarkers. This study will investigate the use of NG-IVIM as a biomarker for treatment response. In the literature, some studies found that NG-IVIM is a significant relevant biomarker. However, most of the research is not corrected for HPV status or consists mainly of HPV-positive cases, which is contradictory when looking at the prognosis of both groups. This study will focus on HPV-negative OPSCC.

The concept of apparent diffusion coefficient (ADC) was introduced in 1986 by Le Bihan et al. [19]. ADC is an estimate of extracellular diffusion. However, it is contaminated by other fluid movements, such as perfusion and intracellular diffusion. If diffusion is the only motion present, the ADC is equal to the diffusion coefficient (D). A low ADC or D indicates a high tissue density. Two years later in 1988, Le Bihan [20] showed an extension on the ADC model with intra-voxel incoherent motion (IVIM). With IVIM it was possible to measure D, but also the pseudo diffusion coefficient (D^*) and the perfussion fraction (f) that are both related to blood flow [21]. D^* is related to the speed of blood and the structure of the capillaries; thus a change in D^* indicates a change in blood perfusion. Meanwhile, f represents the blood volume in the tissue, a change in f thus indicates a difference in the abundance of blood [21]. A further expansion on the IVIM model was proposed by Jensen et al. [22] in 2005 with the non-gaussion Intravoxel Incoherent Motion (NG-IVIM) model. This added kurtosis (K) to the model, now able to measure D,D^*,f and K. K quantifies the deviation from a Gaussian distribution in diffusion-weighted imaging (DWI) and provides insight into tissue complexity and heterogeneity. When diffusion is limited by complex or heterogeneous cell structures, K will be higher[21].

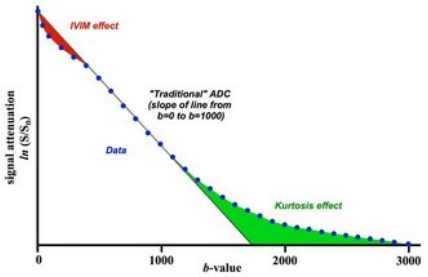

Figure 1.1: The NG-IVIM model as function of the b-value [18]

Research has been done on the influence of pretreatment DWI parameters on treatment outcome; however, they did not correct for HPV status. Multiple studies have found that ADC is a significant predictor of treatment outcome with lower values for patients who responded well to treatment [23, 24, 25, 26, 27, 28, 29, 30, 31]. In a study by Marzi et al. [32] found that at pretreatment D and ADC were significantly lower pretreatment for patients who responded well to therapy. Another study by Hauser et al. [33] concluded that a high initial f may be a predictor of a poor treatment outcome. Some studies have corrected for HPV status, such as Martens et al. [34] who also found that low ADC values are a predictor of a good response to treatment in HPV-negative patients. The study by Sijtsema and Lauwers et al. [35] found that at pretreatment D was correlated with response for HPV-negative patients, with higher values for patients who responded well.

Some studies also investigated the change in DWI parameters between pre- and midtreatment, these studies did not correct for HPV status. In a study by El-Habashy et al. [36] and a study by King et al. [27] a significantly higher increase in $\triangle$ADC was found for patients who responded well at two weeks compared to baseline. Furthermore, a study by Trada et al. [37] did weekly measurements and also found that the $\triangle$ ADC showed a significantly higher increase for patients who responded well, with week 3 showing the lowest p-value. The study by Marzi et al. [32] found that $\triangle$ f between pre- and midtreatment was significant, patients who responded well showed an increase compared to a decrease for patients who did not.

The goal of this study was to investigate changes in DWI values over time (pre- and midtreatment) to determine whether one or more of these DWI parameters correlate with response to treatment. By identifying these correlations, treatments could be personalized in the future, achieving better outcomes for patients and reducing side effects. In addition to DWI parameters, the influence of tumor size and tumor shrinkage on treatment outcome has also been investigated. The location in the tumor where the fastest shrinkage occurs has also been determined, which could provide insight into the behavior of HPV-negative OPSCC.

2. Methods

2.1. Patients and treatment

As described in the paper by Verduijn et al. [17], the patients selected for this study had to meet certain inclusion criteria. The period in which patients are included is from August 2020 until May 2023. It must be a HPV-negative OPSCC without metastases at diagnosis (M0), the patient must be at least 18 years old, a current and/or former smoker, the patient must be scheduled for (chemo-)radiotherapy, and the patient has had a successful planning MRI including NG-IVIM. The HPV status was tested using a p16 test, the p16 protein is highly correlated with HPV [38]. If there were any uncertainties regarding the correctness of the p16 test, due to the high false-positive rate of the p16 tests, an additional HPV test was performed. Whenever possible, the result of the HPV test was utilized.

In total, sixteen patients were included, ten of whom had Complete Response (CR) and six Progressive Disease (PD). More information about these patients can be found in Table 2.1. In total, six patients were found to have a left-sided tumor and ten a right-sided tumor.

Table 2.1: Patient characteristics

	CR	**PD**	**Total**
Number of Patients	10	6	16
Mean Age (years)	60.1	56.1	58.6
Sex			
Male	8	5	13
Female	2	1	3
One year outcome			
CR	10	0	10
PD	0	6	6
Local Failure	0	4	4
Regional Failure	0	2	2
Metastasis	0	3	3
Death	0	4	4
Location of tumor			
Left sided	3	3	6
Right sided	7	3	10
Smoker			
Yes	4	3	7
Former	6	3	9
Never	0	0	0
HPV status			
Positive	0	0	0
Negative	10	6	16
T stage			
T1-2	7	0	7
T3-4	3	6	9
N stage			
N0	1	0	1
N+	9	6	15
M stage			
M0	10	6	16
M+	0	0	0
Radiotherapy			
Photons	9	5	14
Protons	1	1	2
Chemotherapy			
Cisplatine	8	4	12
Cetuximab	0	2	2
Carboplatine	1	0	1

2.2. Image acquisition

For imaging, the same scanner was used for all patients, which is important because one of the limitations of diffusion weighted imaging (DWI) is the variation between the scanners, as mentioned by Conolly et al. [39]. The machine used is a 1.5 T GE MR450w in combination with the MR Radiation Oncology Suite coils. A radiotherapy mask is used for immobilization of the patient. In addition, patients received gadolinium as a contrast agent. This study utilized both a T2 weighted scan and a DWI scan (single-shot echo planar imaging, flip angle: 90 degrees TR: 6700 ms; TE: 81.8 ms; FOV: 26 x 26 cm; 4 mm slice thickness; 0.2 mm slice gap, 128 x 128 matrix, acceleration factor 2) included 15 b-values (0, 10, 2x80, 130, 570, 2x770, 2x780, 790, and 4x1500 s/mm^2) acquired in three orthogonal diffusion directions. These b-values and the DWI sequence were optimized in previous work by Sijtsema et al. [40] and were also applied in earlier work by Sijtsema and Lauwers et al. [35].

2.3. Image registration and Gross Tumor Volume delineation

Image Registration was be applied at multiple moments during this study. Before treatment, the patient receives an MRI scan, later termed a pretreatment scan. The gross tumor volume (GTV) was delineated on the pretreatment T2 by an experienced radiation oncologist. These delineations are performed by an expert radiation oncologist. When patients are two weeks into the treatment cycle, they receive another MRI scan, later referred to as midtreatment scan. The T2 from the mid- and pre-session are rigidly registered on each other using the software from MIM using a mutual information metric [41]. When the GTV delineation was transferred between T2 scans, an expert radiation oncologist adjusted it to account for registration inaccuracies and decreased tumor volume as a result of treatment. Each T2 scan was registered with the b=0 image of the same time point, using rigid registration using in-house software, allowing rotation and translation based on the mutual information metric of mattes, developed by Mattes et al. [42]. The GTV's in the b=0 image are checked to ensure that they do not include the air voxels of the trachea; if so, they are removed. In this way, eventually two GTV's are available, one for the pretreatment volume and one for the midtreatment volume. The registration workflow can be seen in Figure 2.1, the normal arrows indicate registration with the in-house software and the dotted lines indicate registration using the MIM software. The reason for the two different methods is that the anatomy changes during the course of treatment and the software from MIM is newer and more advanced than the in-house software.

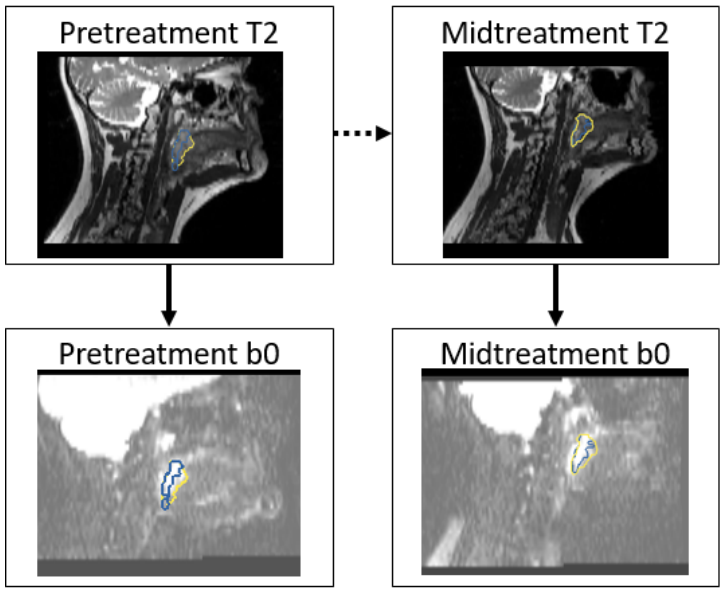

Figure 2.1: Registration pipeline, the normal arrow means registration using in-house software and the dotted arrow is done with MIM software

2.4. Parameter calculation

All parameters were fitted using an in-house developed code in Matlab. For ADC Equation 2.1 was used [19]. For the NG-IVIM paramaters, a more advanced model was used using Equation 2.2 [21].

$$S(b) = S_0 e^{-b \cdot \text{ADC}} \tag{2.1}$$

$$S(b) = S_0 \left[(1-f) \exp\left(-bD + \frac{1}{6} b^2 D^2 K \right) + f \exp\left(-bD^*\right) \right] \tag{2.2}$$

where:

- $S(b)$ is the signal intensity at a given b-value,
- S_0 is the signal intensity without diffusion weighting ($b = 0$),
- ADC is the apparant diffusion coefficient,
- f is the perfusion fraction,
- D is the diffusion coefficient,
- D^* is the pseudo-diffusion coefficient,
- K is the kurtosis,
- b is the diffusion weighting factor.

Using this model, four parameters can be calculated. The pseudo-diffusion coefficient (D^*) and the perfusion fraction (f) are related to blood perfusion. Where D^* is related to the speed of blood and the structure of the capillaries,and f represents the volumes of blood of the tissue. The diffusion coefficient (D) and kurtosis (K) are related to the diffusion of water. where D characterizes the mobility of water molecules and K describes the deviation from the Gaussian distribution and tells something about the complexity and heterogeneity of the tissue [21].

The fitting model had predefined ranges, with the lower bound preventing negative values and both the lower and upper bounds ensuring physical plausibility. These ranges are described in the Appendix B.

Furthermore, the tumor size was also determined by multiplying the amount of voxels in the GTV with their voxelsize. This was done for both pretreatment and midtreatment and was split according to response to treatment.

2.5. Response assessment

For this study, treatment response was scored based on a one-year follow-up which consisted of clinical evaluation and MR imaging, when necessary. During the first year after radiotherapy, follow-up appointments were carried out every two months. PD is defined as local disease, regional disease, distant metastasis, and/or death related to the original tumor. CR was characterized by the absence of PD.

2.6. Parameter analysis

The mean inside the GTV structure is taken for each patient, parameter and time point. By comparing the mean values of the CR and PD groups with each other, information can be gained about the micro structure of the tumor. The groups were analyzed at each time point, but the changes between mid- and pretreatment have also been analyzed in absolute and relative form.

Furthermore, the midtreatment GTV is registered on the pretreatment scan. Using the two GTV's on the pretreatment scan, three regions can be created, the pretreatment GTV, the midtreatment GTV, and the area between them by subtracting the midtreatment GTV from the pretreatment GTV. In this way, it can be investigated whether the tumor tissue that remains after two weeks has different characteristics at the pretreatment moment compared to the tumor tissue that has disappeared and therefore may be more radio sensitive. The CR and PD groups are treated as separate groups here as well.

2.7. Tumor shrinkage

Using the pre- and midtreatment GTV's registered on each other, an analysis has been done on how the tumor shrinks. First, tumor shrinkage has been determined by calculating the absolute and relative differences in GTV volume at the two time points. A distinction has been made between CR and PD to see if one of the groups shows more shrinkage after two weeks of therapy.

2.8. Tumor shrinkage location

An analysis has been done on the location of shrinkage. Distinguishing between left and right sided tumors was preferred over categorizing into CR and PD, due to the importance of the tumor's position relative to the trachea. The interest lies in the shrinkage direction in relation to the trachea, which differs for left and right sided tumors. The position of the tumor is determined by looking at the center of volume of the pretreatment GTV and comparing this to the center of volume of the spinal cord, which was also delineated as part of the treatment process.

Using the center of volume of the pretreatment GTV as the central point, eight regions have been created around this. The center of volume is used as a new reference point for a coordinate system from which eight regions can be created, left/right, front/back, and bottom/top. Each left sided and right sided region was added together. The left sided region of the right sided tumors was categorized into a new group together with the right sided region of the left sided tumors, this group represents the group near the trachea. In the same way, the left sided region of left sided tumors and the right sided region of right sided tumors were added to a group representing the regions closer to the skin. The shrinkage between mid- and pretreatment has been calculated. This is done to see if certain areas have tendencies to shrink faster.

2.9. Statistics

The statistical methods used during this study are the Mann-Whitney U-test and the Wilcoxon signed-rank test. The Mann-Whitney U-test can be used to test whether there is a rank sum difference between two groups and is the non-parametric counterpart of the t-test. The test also assumes that there is no normal distribution in the data [43]. The Wilcoxon signed-rank test the mean values of two dependent groups, so paired data, for example, from the same patient. Like the Mann-Whitney U-test, the Wilcoxon signed-rank test is also non-parametric and does not require normal distributed data [44]. In each section of the results, the method used is mentioned as a result of the data being paired or not. The result was considered statistically significant when the p-value was less than 0.05 ($p < 0.05$). The Mannwhitneyu and Wilcoxon function of SciPy was used for the calculations [45, 46]. During this study, no corrections have been made for multiple testing.

3. Results

3.1. Analysis of Mean Parameter Values and Changes Over Time

In Figure C.2, from Appendix C, the mean values of each parameter are shown for CR and PD on the pre- and midtreatment scans. Statistics are applied to see if there is a significant difference in mean at a certain time point between CR and PD. The parameters with the p-value are also shown in Table 3.1, no significant differences were found. Furthermore, the change over time was also calculated, absolute and relative, to determine whether there is a difference between the two groups of patients. These results are also shown in table 3.1. Absolute and relative changes in D have been shown to be significant, p = 0.017 and p = 0.029, respectively. In both cases CR showed a decrease in D and PD an increase. The results can be seen in Figure 3.1. The results for absolute differences can be seen in Figure C.1 from Appendix C. For this section, the Mann-Whitney U-test was used, as described in Section 2.9.

3.2. Tumor size

An additional interesting parameter is the size of the tumor. This is calculated on the basis of the GTV. In both pre- and midtreatment measurements, a significant difference between CR and PD was observed. With a tumor size of $(3.5 \pm 3.0) \cdot 10^3$ mm^3 vs $(8.9 \pm 6.6) \cdot 10^3$ mm^3 and a p value of 0.037 for pretreatment, and $(2.2 \pm 2.0) \cdot 10^3$ mm^3 vs $(7.3 \pm 5.1) \cdot 10^3$ mm^3 and a p value of 0.017 for midtreatment. The results can be seen in Figure 3.2, for this section the Mann-Whitney U-test was used, as described in Section 2.9.

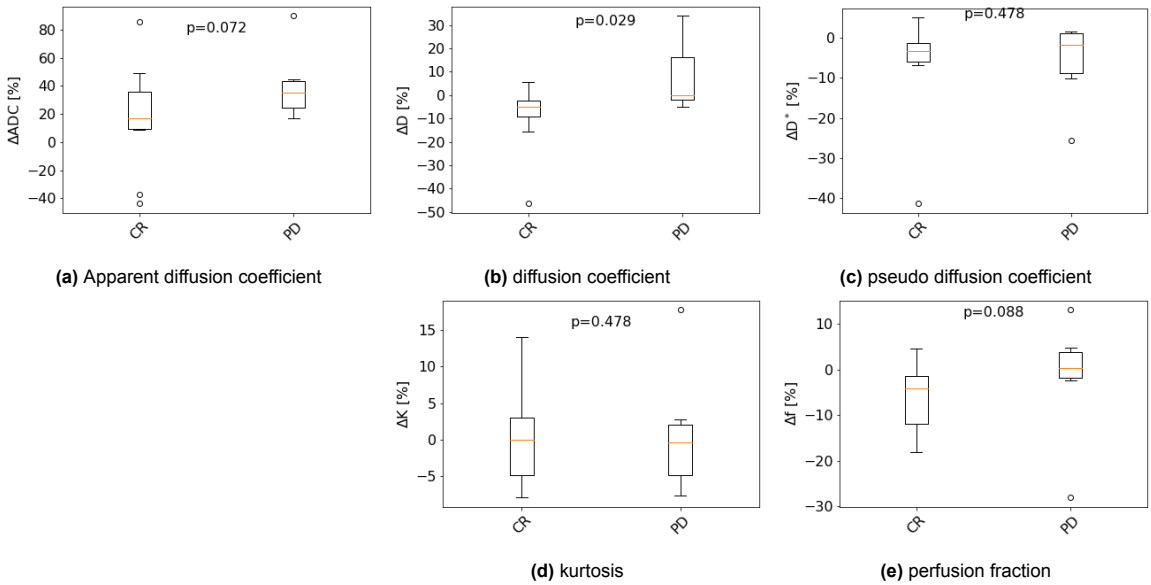

(a) Apparent diffusion coefficient

(b) diffusion coefficient

(c) pseudo diffusion coefficient

(d) kurtosis

(e) perfusion fraction

Figure 3.1: The percentage difference between the pretreatment and midtreatment scans divided between Complete response, CR (n = 10) and Progressive disease, PD (n = 6). For the ADC and NG-IVIM parameters.

Table 3.1: Results from the tumor mean measurements. Shown is the mean of the Complete Response (CR) and Progressive Disease(PD) patient group with the standard deviation. For the ADC and NG-IVIM parameters.

		Pretreatment	Midtreatment	Absolute change	Relative change(%)
ADC	CR	1.57 ± 0.93	1.62 ± 0.48	0.06 ± 0.72	17.3 ± 36.3
$\cdot 10^{-3}$ [mm^{2}s^{-1}]	PD	1.13 ± 0.15	1.57 ± 0.22	0.44 ± 0.23	40.6 ± 23.9
	p-value	0.151	0.275	0.127	0.072
D	CR	1.58 ± 0.76	1.35 ± 0.29	-0.23 ± 0.51	-8.8 ± 13.7
$\cdot 10^{-3}$ [mm^{2}s^{-1}]	PD	1.23 ± 0.17	1.33 ± 0.30	0.11 ± 0.19	8.0 ± 14.6
	p-value	0.127	0.435	**0.017**	**0.029**
D*	CR	2.86 ± 1.18	2.62 ± 1.04	-0.24 ± 0.6	-6.2 ± 12.2
$\cdot 10^{-2}$ [mm^{2}s^{-1}]	PD	2.44 ± 0.48	2.29 ± 0.53	-0.15 ± 0.24	-6.1 ± 9.7
	p-value	0.435	0.352	0.478	0.478
f	CR	0.218 ± 0.081	0.204 ± 0.072	-0.015 ± 0.019	-6.5 ± 7.4
[-]	PD	0.200 ± 0.036	0.195 ± 0.041	-0.005 ± 0.029	-2.0 ± 12.8
	p-value	0.435	0.478	0.088	0.088
k	CR	0.766 ± 0.164	0.770 ± 0.173	0.004 ± 0.057	0.7 ± 6.7
[-]	PD	0.800 ± 0.044	0.810 ± 0.098	0.010 ± 0.067	1.0 ± 8.4
	p-value	0.478	0.478	0.435	0.478

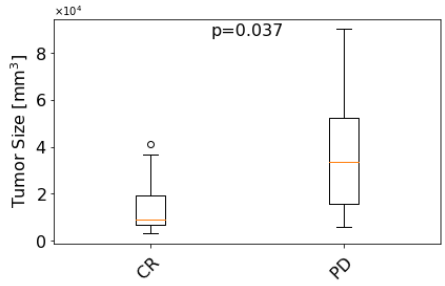

(a) Pretreatment tumor size

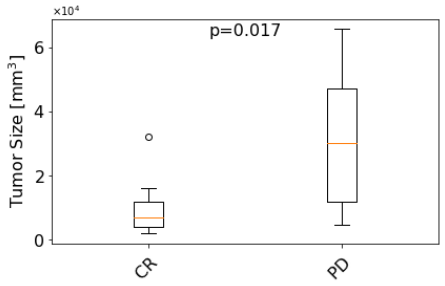

(b) Midtreatment tumor size

Figure 3.2: Tumor size at pre- and midtreatment for both Complete Response (CR) and Progressive Disease(PD). (a) shows the sizes at pretreatment and (b) the sizes at midtreatment

3.3. Tumor heterogeneity

The region that showed a reduction after two weeks of radiotherapy was tested for differences compared to the tissue that remained after two weeks. In Figure 3.3 is an example of a T2 scan of a patient. In this figure, the pretreatment GTV is marked in orange, and the midtreatment GTV is marked in purple. Patients were split according to their response. The parameters were calculated based on the pretreatment DWI scan, and two regions are distinguished:

- The midtreatment volume, everything within the purple GTV
- The tissue between the two GTV's, representing the margin that is gone after two weeks

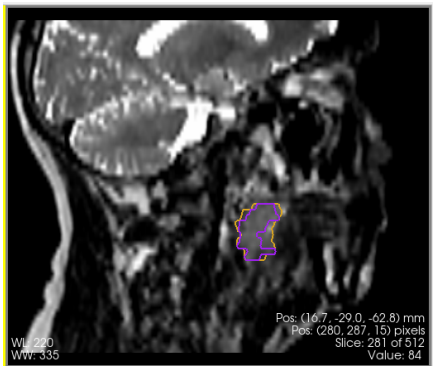

Figure 3.3: A slice of a T2 scan, orange indicates the pretreatment GTV and purple the midtreatment GTV

The resulting box plots can be seen in Figure D.1 from Appendix D. The data is shown in Table 3.2. It can be seen that for CR ADC,D and f showed significant differences, for these three parameters, the values for the region that disappeared are higher. For PD only f was significant, again showing a higher value for the region that has disappeared. For this section, the Wilcoxon signed-rank test was used, as described in Section 2.9.

Table 3.2: Mean region results from the regions based on pretreatment scan data. Shown is the mean of the Complete Response (CR) and Progressive Disease(PD) patient group with the standard deviation. For the ADC and NG-IVIM parameters.

		residu at 2 weeks	**clean at 2 weeks**	**p-value**
ADC	CR	1.44 ± 0.88	1.69 ± 0.93	**0.005**
$\cdot 10^{-3}$ (mm^2s^{-1})	PD	1.11 ± 0.16	1.19 ± 0.13	0.173
D	CR	1.48 ± 0.77	1.67 ± 0.70	**0.037**
$\cdot 10^{-3}$ (mm^2s^{-1})	PD	1.19 ± 0.19	1.28 ± 0.10	0.345
D*	CR	2.75 ± 1.10	2.97 ± 1.18	0.074
$\cdot 10^{-2}$ (mm^2s^{-1})	PD	2.44 ± 0.46	2.54 ± 0.51	0.249
f	CR	0.203 ± 0.076	0.241 ± 0.081	**0.007**
(-)	PD	0.195 ± 0.034	0.220 ± 0.042	**0.046**
K	CR	0.768 ± 0.160	0.794 ± 0.193	0.721
(-)	PD	0.800 ± 0.047	0.853 ± 0.103	0.463

3.4. Tumor shrinkage

Tumor shrinkage was also determined and compared between CR and PD. These results can be seen in Figure 3.4. Although not significant, there appears to be a large difference between the averages of the two groups with a value of -30.8 $\pm$ 20.7 % versus -18.4 $\pm$ 8.6 % with p=0.106 relatively and $(-5 \pm 7) * 10^3$ versus $(-7 \pm 8) * 10^3$ with p=0.313 absolutely. For this section, the Mann-Whitney U-test was used, as described in Section 2.9.

(a) Absolute change in tumor size

(b) Relative change in tumor size

Figure 3.4: Tumor size change between pre- and midtreatment in both Complete Response (CR) and Progressive Disease(PD). (a) shows the absolute change and (b) the relative change.

3.5. Tumor shrinkage location

It was tested where the tumor would shrink the fastest over time. For this, the center of volume was used of the pretreatment GTV, around this point eight new regions were created; back/front, left/right, bottom/top. For each region, the shrinkage between pretreatment and midtreatment was determined. Based on the center of volume the tumors compared to the spinal cord were split into left (n = 6) and right (n = 10) tumors. The results of this can be seen in figures E.1 and E.2 in appendix E. To test whether there is a difference between the left and right sided regions, these regions were added together. The resulting results can be seen in figures 3.5 and 3.6. For left and right tumors, there was no significant change in volume on the left side of the tumor compared to the right side, with p = 0.249

and p = 0.059, respectively. However, the results can be added together. Because, the left side of a left sided tumor has the same meaning as the right side of a right sided tumor, both are on the outside and closer to the skin than the trachea. The other way around, the right side of a left sided tumor and the left side of a right sided tumor are closer to the trachea. In this way a distinction is made between the side closer to the skin and the side closer to the trachea, which can be seen in Figure 3.7. The side near the trachea had a decrease of -17±25 % compared to -30±19 % for the skin side, with a significant p-value of 0.039. Here, the Wilcoxon signed-rank test is applied because the data is paired.

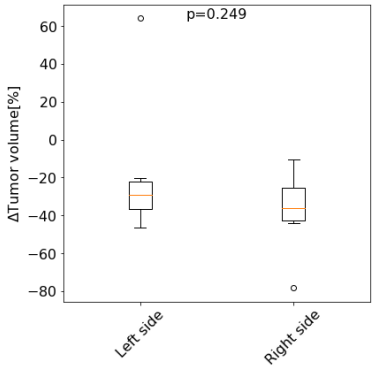

Figure 3.5: Tumor shrinkage for left sided tumors. The tumor is split in a left and right side

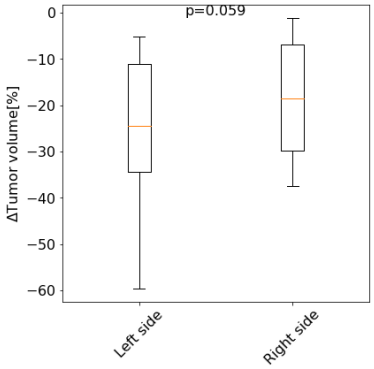

Figure 3.6: Tumor shrinkage for right sided tumors. The tumor is split in a left and right side

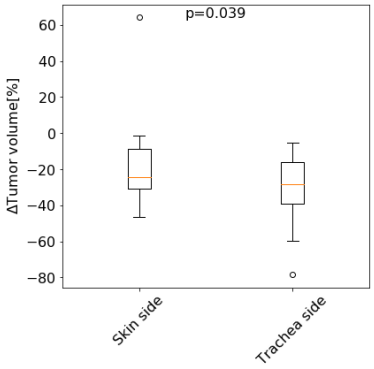

Figure 3.7: Tumor shrinkage combined and split between a side near the skin and a side near the trachea

4. Discussion

In this study, the influence of DWI parameters on treatment outcome has been studied and several tumor characteristics such as heterogeneity and shrinkage have been studied. This has been done for a group of sixteen HPV-negative OPSCC patients. The treatment response in one year was determined and divided between CR and PD, with ten and six patients in each group, respectively. Of the NG-IVIM parameters, D^* and f, are related to blood perfusion. The other parameters, D and K, are related to the diffusion of water in tissues [21].

None of the DWI parameters differed significantly between CR and PD in our study at pre- and midtreatment. This result contradicts other studies done. In studies that did not correct for HPV status, significant results have been found, as in the study by Freihat et al. [23]. ADC was found to be a significant predictor at pretreatment, with PD showing higher values. More studies have also related a high ADC value to worse treatment outcomes [47, 24, 25, 26, 27, 28, 29, 30, 31]. Martens et al. [34] corrected for HPV status and also found that high ADC values are a predictor of PD in HPV-negative patients. In the study by Lauwers and Sijtsema et al. [35], where a correction for HPV status was made, D was found to be a predictor at pretreatment with CR patients showing a higher value, for HPV-negative patients. In our study, both ADC and D showed higher values for CR at pretreatment, although not significant. The reason for this could be the low number of patients. During the course of this study, it was found that the results could change a lot when an additional patient was included. This shows the importance of including more patients. The higher values for both ADC and D are counter intuitive, but could be due to HPV status. As a study by Driessen et al. [48] showed, ADC values are correlated with HPV status. More studies are required for HPV-negative OPSC to explore the role of DWI parameters in predicting treatment response accurately and to uncover the underlying mechanisms that influence these parameters.

The difference between pre- and midtreatment was investigated in relative and absolute terms, here it was found that D was a significant predictor with $p = 0.017$ for the absolute difference and $p = 0.029$ for the relative differences between CR and PD, showing a increase for PD and a decrease for CR. In studies that did not correct for HPV status, it was found that patients with CR had a significantly greater increase in ADC than patients with PD [30, 27, 36, 37], for D the same was found [49]. A study by Marzi et al. [32] found that differences in f were a predictor, showing an increase for CR and a decrease for PD. In our study, it was found that CR had a larger decrease than PD, with a p-value of 0.088. A decrease in f could indicate tissue necrosis [50], indicating therapeutic success. In the study by Marzi et al. [32], they did not find that the difference in D was significant. Their study used a small mixed group, with respect to HPV status, of 12 patients. In addition, midtreatment was defined at 3 weeks, instead of 2 weeks as in our study. The latter is of importance, as shown by Trada et al. [37], where weekly DWI scans were performed in a group with mostly unknown HPV status. Here, they found that compared to baseline, week three performed best with a significant relative difference in ADC with a p-value of 0.003 compared to 0.019 at two weeks. In both studies a 1.5T scanner was used like in our study. By defining midtreatment at three weeks it could have been possible that the results of this study showed more significant results. However, if eventually applied in the clinic, this would also postpone treatment alterations by a week.

The size of the tumor was also found to be a predictive factor. Patients with PD showed significantly larger tumors prior and during treatment with a p-value of 0.037 and 0.017 respectively. This makes sense because T in the TNM staging is related to the size of the tumor [51], and a higher T-stage is associated with lower overall survival [52]. The results at midtreatment have shown to be more significant than at pretreatment, suggesting that midtreatment tumor size could potentially be used as a predictor

of treatment response. In addition, a larger decrease in tumor volume has been found in CR and PD, although not significant. However, the results were promising and the addition of more patients could be beneficial. Paudyal et al. [49] found a similar result, who showed that volume change at one week could already be a significant indicator with a greater decrease in CR.

When comparing the residual part of the tumor with the disappeared part according to pretreatment parameters, it was found that for patients with CR, a significantly higher value was found for ADC,D and f in the region that has disappeared at 2 weeks. For patients with PD, this was only the case for f. Indicating that there appear to be significant differences in tissue characteristics in these regions. The reasons for this difference could be due to the number of patients in each group, with PD having only six patients and CR ten. A higher ADC,D, and f would indicate a lower cell density and more blood present. The presence of more blood could indicate that there is also more oxygen available, oxygen is necessary to induce DNA damage in the cancer cell which could lead to cell death [53]. This, in turn, results in a higher oxygen enhancement ratio [54]. This could explain why this area showed a reduction. In addition, the edges on the GTV are of great importance for this test and due to delineation uncertainty these results are affected as well. Differences in anatomy could also be the reason for these results, because of the chaotic nature of tumor blood vessels it can be that the outer edges of a tumor are better accessible than the inner part.

The shrinkage of the tumor has also been studied in comparison to its location in the human body. It was found that for left- and right-sided tumors there was no significant difference in shrinkage of the left and right side of the tumor itself. However, when added together, and the tumors are divided into a half on the skin side and a half on the trachea side, it was found that the half near the trachea showed a significantly higher reduction with a p-value of 0.039. This potentially benefits the patient because breathing will become more and more easier during the course of treatment.

The limitations of this study are the small group of patients and the short follow-up period. In addition, there has been no correction for multiple testing due to the small group of patients. Due to these limitations, the results found in this study would not be sufficient to support a decision-making model for patients in the clinic. The outcome in case of suspicion of PD would be giving a higher dose or stopping radiotherapy, both of which come with severe consequences, and decisions such as these must be made with a lot of care, considering the quality of life and risks involved. It is essential to include more patients to reach a level of certainty for making these decisions, along with the integration of more biomarkers, which is the goal of the COMPLETE trial.

5. Conclusion

This study investigated the influence of DWI parameters on treatment outcomes in sixteen patients with HPV-negative OPSCC. No significant differences in DWI parameters were observed between CR and PD at pre- and midtreatment, contradicting previously performed studies. The small group of patients and the short follow-up are probably the reasons for the lack of significant findings.

In this study, the change in D between pre- and midtreatment was found to be a significant predictor for treatment response, both absolute and relative. A larger increase for PD was found compared to CR. This contradicts other studies which did not have corrected for HPV status, there a larger increase for CR was found.

This study also found that analysis of pretreatment parameters revealed a significant difference in ADC, D and f for CR, as well as f for PD, when comparing the residual region to the region that had after two weeks. In this study a higher reduction has also been found in the side of the tumors near the trachea compared to the side near the skin, potentially improving the patient's breathing during treatment.

In conclusion, while DWI parameters and tumor size have shown potential as biomarkers for treatment response in HPV-negative OPSCC, more research with larger cohorts and additional biomarkers is needed to develop reliable clinical decision-making tools.

References

[1] *AI Image Generator - Create Art, Images and Video | Leonardo AI*. URL: https://leonardo.ai/.

[2] E Chimenos-Küstner, MS Marques-Soares, and M Schemel-Suárez. "Consideraciones sobre etiopatogenia y prevención del cáncer orofaríngeo". In: *Medicina de Familia. SEMERGEN* 45.7 (2019), pp. 497–503.

[3] Takafumi Nakagaki et al. "Targeted next-generation sequencing of 50 cancer-related genes in Japanese patients with oral squamous cell carcinoma". In: *Tumor Biology* 40.9 (2018), p. 1010428318800180.

[4] Susanne Flach et al. "Analysis of genetic variants of frequently mutated genes in human papillomavirus-negative primary head and neck squamous cell carcinoma, resection margins, local recurrences and corresponding circulating cell-free DNA". In: *Journal of Oral Pathology & Medicine* 51.8 (2022), pp. 738–746.

[5] Jon Mork et al. "Human papillomavirus infection as a risk factor for squamous-cell carcinoma of the head and neck". In: *New England Journal of Medicine* 344.15 (2001), pp. 1125–1131.

[6] Paolo Boscolo-Rizzo et al. "Rising Trend in the Prevalence of HPV-Driven Oropharyngeal Squamous Cell Carcinoma during 2000–2022 in Northeastern Italy: Implication for Using p16INK4a as a Surrogate Marker for HPV-Driven Carcinogenesis". In: *Cancers* 15.9 (May 2023), pp. 2643–2643. DOI: https://doi.org/10.3390/cancers15092643. URL: https://www.ncbi.nlm.nih.gov/pmc/articles/PMC10177129/.

[7] Henrike Reder et al. "Plasma cell-free human papillomavirus oncogene E6 and E7 DNA predicts outcome in oropharyngeal squamous cell carcinoma". In: *The Journal of Molecular Diagnostics* 22.11 (2020), pp. 1333–1343.

[8] Sarah Tadhg Ferrier et al. "Blood and saliva-derived ctDNA is a marker of residual disease after treatment and correlates with recurrence in human papillomavirus-associated head and neck cancer". In: *Cancer Medicine* 12.15 (2023), pp. 15777–15787.

[9] Alok R Khandelwal et al. "Comparing cell-free circulating tumor DNA mutational profiles of disease-free and nonresponders patients with oropharyngeal squamous cell carcinoma". In: *Laryngoscope Investigative Otolaryngology* 5.5 (2020), pp. 868–878.

[10] Sana Batool et al. "Circulating tumor-tissue modified HPV DNA testing in the clinical evaluation of patients at risk for HPV-positive oropharynx cancer: The IDEA-HPV study". In: *Oral Oncology* 147 (2023), p. 106584.

[11] Denis Soulieres et al. "Molecular alterations and buparlisib efficacy in patients with squamous cell carcinoma of the head and neck: biomarker analysis from BERIL-1". In: *Clinical cancer research* 24.11 (2018), pp. 2505–2516.

[12] Bhishamjit S Chera et al. "Rapid clearance profile of plasma circulating tumor HPV type 16 DNA during chemoradiotherapy correlates with disease control in HPV-associated oropharyngeal cancer". In: *Clinical Cancer Research* 25.15 (2019), pp. 4682–4690.

[13] Michael M Allevato et al. "Tumor-derived exosomes and the role of liquid biopsy in human papillomavirus oropharyngeal squamous cell carcinoma". In: *The Cancer Journal* 29.4 (2023), pp. 230–237.

[14] Yifan Xu et al. "Hypermethylation of nc886 in HPV-positive oropharyngeal cancer and its clinical implications: An epigenome-wide association study". In: *Molecular Therapy-Nucleic Acids* 30 (2022), pp. 596–605.

[15] Stephanie G Craig et al. "Recommendations for determining HPV status in patients with oropharyngeal cancers under TNM8 guidelines: a two-tier approach". In: *British Journal of Cancer* 120.8 (2019), pp. 827–833.

[16] *Cancerresearchuk.org*. June 2024. URL: https://www.cancerresearchuk.org/about-cancer/treatment/radiotherapy/side-effects/head-and-neck-radiotherapy-side-effects.

[17] Gerda M Verduijn et al. "The COMPLETE trial: HolistiC early respOnse assessMent for oroPharyngeaL cancEr paTiEnts; Protocol for an observational study". In: *BMJ open* 12.5 (May 2022), e059345–e059345. DOI: https://doi.org/10.1136/bmjopen-2021-059345. URL: https://pubmed.ncbi.nlm.nih.gov/35584883/.

[18] *Questions and Answers in MRI*. 2015. URL: https://mriquestions.com/ivim.html.

[19] D Le Bihan et al. “MR imaging of intravoxel incoherent motions: application to diffusion and perfusion in neurologic disorders.” In: *Radiology* 161.2 (Nov. 1986), pp. 401–407. DOI: https://doi.org/10.1148/radiology.161.2.3763909. URL: https://pubmed.ncbi.nlm.nih.gov/3763909/.

[20] D. Le Bihan. “Intravoxel incoherent motion imaging using steady□state free precession”. In: *Magnetic resonance in medicine* 7.3 (July 1988), pp. 346–351. DOI: https://doi.org/10.1002/mrm.1910070312. URL: https://pubmed.ncbi.nlm.nih.gov/3205150/.

[21] Yonggang Lu et al. “Extension of the intravoxel incoherent motion model to non□gaussian diffusion in head and neck cancer”. In: *Journal of magnetic resonance imaging* 36.5 (July 2012), pp. 1088–1096. DOI: https://doi.org/10.1002/jmri.23770. URL: https://pubmed.ncbi.nlm.nih.gov/22826198/.

[22] Jens H Jensen et al. “Diffusional kurtosis imaging: The quantification of non□gaussian water diffusion by means of magnetic resonance imaging”. In: *Magnetic resonance in medicine* 53.6 (May 2005), pp. 1432–1440. DOI: https://doi.org/10.1002/mrm.20508. URL: https://onlinelibrary.wiley.com/doi/10.1002/mrm.20508.

[23] Omar Freihat et al. “Pre-treatment PET/MRI based FDG and DWI imaging parameters for predicting HPV status and tumor response to chemoradiotherapy in primary oropharyngeal squamous cell carcinoma (OPSCC)”. In: *Oral oncology* 116 (May 2021), pp. 105239–105239. DOI: https://doi.org/10.1016/j.oraloncology.2021.105239. URL: https://www.sciencedirect.com/science/article/pii/S1368837521000622?via%3Dihub.

[24] Masamitsu Hatakenaka et al. “Pretreatment Apparent Diffusion Coefficient of the Primary Lesion Correlates With Local Failure in Head-and-Neck Cancer Treated With Chemoradiotherapy or Radiotherapy”. In: *International Journal of Radiation Oncology*Biology*Physics* 81.2 (Oct. 2011), pp. 339–345. DOI: https://doi.org/10.1016/j.ijrobp.2010.05.051. URL: https://www.redjournal.org/article/S0360-3016(10)00795-9/abstract.

[25] Kayoko Ohnishi et al. “Prediction of Local Failures with a Combination of Pretreatment Tumor Volume and Apparent Diffusion Coefficient in Patients Treated with Definitive Radiotherapy for Hypopharyngeal or Oropharyngeal Squamous Cell Carcinoma”. In: *Journal of Radiation Research* 52.4 (Jan. 2011), pp. 522–530. DOI: https://doi.org/10.1269/jrr.10178. URL: https://academic.oup.com/jrr/article/52/4/522/1052938.

[26] Ashok Srinivasan et al. “Utility of Pretreatment Mean Apparent Diffusion Coefficient and Apparent Diffusion Coefficient Histograms in Prediction of Outcome to Chemoradiation in Head and Neck Squamous Cell Carcinoma”. In: *Journal of Computer Assisted Tomography* 36.1 (Jan. 2012), pp. 131–137. DOI: https://doi.org/10.1097/rct.0b013e3182405435. URL: https://journals.lww.com/jcat/abstract/2012/01000/utility_of_pretreatment_mean_apparent_diffusion.21.aspx.

[27] Ann D King et al. “Head and Neck Squamous Cell Carcinoma: Diagnostic Performance of Diffusion-weighted MR Imaging for the Prediction of Treatment Response”. In: *Radiology* 266.2 (Feb. 2013), pp. 531–538. DOI: https://doi.org/10.1148/radiol.12120167. URL: https://pubmed.ncbi.nlm.nih.gov/23151830/.

[28] Sanjeev Chawla et al. “Pretreatment Diffusion-Weighted and Dynamic Contrast-Enhanced MRI for Prediction of Local Treatment Response in Squamous Cell Carcinomas of the Head and Neck”. In: *American Journal of Roentgenology* 200.1 (Jan. 2013), pp. 35–43. DOI: https://doi.org/10.2214/ajr.12.9432. URL: https://www.ajronline.org/doi/full/10.2214/AJR.12.9432.

[29] Maarten Lambrecht et al. “Integrating pretreatment diffusion weighted MRI into a multivariable prognostic model for head and neck squamous cell carcinoma”. In: *Radiotherapy and Oncology* 110.3 (Mar. 2014), pp. 429–434. DOI: https://doi.org/10.1016/j.radonc.2014.01.004. URL: https://www.thegreenjournal.com/article/S0167-8140(14)00009-7/abstract.

[30] Daniel P Noij et al. “Predictive value of diffusion-weighted imaging without and with including contrast-enhanced magnetic resonance imaging in image analysis of head and neck squamous cell carcinoma”. In: *European Journal of Radiology* 84.1 (Jan. 2015), pp. 108–116. DOI: https://doi.org/10.1016/j.ejrad.2014.10.015. URL: https://www.ejradiology.com/article/S0720-048X(14)00480-X/fulltext.

[31] Mariangela Lombardi et al. “Predictive value of pre-treatment apparent diffusion coefficient (ADC) in radiochemiotherapy treated head and neck squamous cell carcinoma”. In: *La radiologia medica* 122.5 (Feb. 2017), pp. 345–352. DOI: https://doi.org/10.1007/s11547-017-0733-y. URL: https://link.springer.com/article/10.1007/s11547-017-0733-y.

[32] Simona Marzi et al. “The prediction of the treatment response of cervical nodes using intravoxel incoherent motion diffusion-weighted imaging”. In: *European journal of radiology* 92 (July 2017), pp. 93–102. DOI: https://doi.org/10.1016/j.ejrad.2017.05.002. URL: https://www.sciencedirect.com/science/article/pii/S0720048X17301742?via%3Dihub.

[33] Thomas Hauser et al. “Characterization and therapy monitoring of head and neck carcinomas using diffusion-imaging-based intravoxel incoherent motion parameters—preliminary results”. In: *Neuroradiology* 55.5 (Feb. 2013), pp. 527–536. DOI: https://doi.org/10.1007/s00234-013-1154-9. URL: https://pubmed.ncbi.nlm.nih.gov/23417120/.

[34] Roland M Martens et al. “Predictive value of quantitative diffusion-weighted imaging and 18-F-FDG-PET in head and neck squamous cell carcinoma treated by (chemo)radiotherapy”. In: *European Journal of Radiology* 113 (Apr. 2019), pp. 39–50. DOI: https://doi.org/10.1016/j.ejrad.2019.01.031. URL: https://pubmed.ncbi.nlm.nih.gov/30927958/.

[35] Nienke D Sijtsema et al. “Relating pre-treatment Non-Gaussian Intravoxel Incoherent Motion Diffusion-Weighted imaging to human papillomavirus status and response in oropharyngeal carcinoma”. In: *Physics and imaging in radiation oncology* 30 (Apr. 2024), pp. 100574–100574. DOI: https://doi.org/10.1016/j.phro.2024.100574. URL: https://pubmed.ncbi.nlm.nih.gov/38633282/.

[36] Dina M El-Habashy et al. “Longitudinal diffusion and volumetric kinetics of head and neck cancer magnetic resonance on a 1.5T MR-Linear accelerator hybrid system: A prospective R-IDEAL Stage 2a imaging biomarker characterization/ pre-qualification study”. In: *medRxiv (Cold Spring Harbor Laboratory)* (May 2023). DOI: https://doi.org/10.1101/2023.05.04.23289527. URL: https://pubmed.ncbi.nlm.nih.gov/37205359/.

[37] Yuvnik Trada et al. “Changes in serial multiparametric MRI and FDG-PET/CT functional imaging during radiation therapy can predict treatment response in patients with head and neck cancer”. In: *European radiology* 33.12 (July 2023), pp. 8788–8799. DOI: https://doi.org/10.1007/s00330-023-09843-2. URL: https://pubmed.ncbi.nlm.nih.gov/37405500/.

[38] Josena K Stephen et al. “Significance of p16 in site-specific HPV positive and HPV negative HNSCC”. In: *Cancer and clinical oncology* 2.1 (Dec. 2012). DOI: https://doi.org/10.5539/cco.v2n1p51. URL: https://pubmed.ncbi.nlm.nih.gov/23935769/.

[39] Michael Connolly and Ashok Srinivasan. “Diffusion-Weighted Imaging in Head and Neck Cancer”. In: *Magnetic resonance imaging clinics of North America* 26.1 (Feb. 2018), pp. 121–133. DOI: https://doi.org/10.1016/j.mric.2017.08.011. URL: https://www.sciencedirect.com/science/article/pii/S1064968917300995?via%3Dihub.

[40] Nienke D Sijtsema et al. “An optimal acquisition and post□processing pipeline for hybrid IVIM□DKI in head and neck”. In: *Magnetic resonance in medicine* 85.2 (Aug. 2020), pp. 777–789. DOI: https://doi.org/10.1002/mrm.28461. URL: https://onlinelibrary.wiley.com/doi/epdf/10.1002/mrm.28461?src=getftr.

[41] *Mimsoftware.com*. URL: https://www.mimsoftware.com/radiation-oncology/mim-maestro/image-registration.

[42] D Mattes et al. “PET-CT image registration in the chest using free-form deformations”. In: *IEEE transactions on medical imaging* 22.1 (Jan. 2003), pp. 120–128. DOI: https://doi.org/10.1109/tmi.2003.809072. URL: https://ieeexplore.ieee.org/document/1191368.

[43] *Datatab.net*. URL: https://datatab.net/tutorial/mann-whitney-u-test.

[44] *Datatab.net*. URL: https://datatab.net/tutorial/wilcoxon-test.

[45] *Scipy.org*. URL: https://docs.scipy.org/doc/scipy/reference/generated/scipy.stats.mannwhitneyu.html.

[46] URL: https://docs.scipy.org/doc/scipy/reference/generated/scipy.stats.wilcoxon.html.

[47] M. Ravanelli et al. “Pretreatment DWI with Histogram Analysis of the ADC in Predicting the Outcome of Advanced Oropharyngeal Cancer with Known Human Papillomavirus Status Treated with Chemoradiation”. In: *American journal of neuroradiology* 41.8 (July 2020), pp. 1473–1479. DOI: https://doi.org/10.3174/ajnr.a6695. URL: https://pubmed.ncbi.nlm.nih.gov/32732272/.

[48] Juliette P Driessen et al. “Correlation of human papillomavirus status with apparent diffusion coefficient of diffusion□weighted MRI in head and neck squamous cell carcinomas”. In: *Head and neck* 38.S1 (July 2015). DOI: https://doi.org/10.1002/hed.24051. URL: https://pubmed.ncbi.nlm.nih.gov/25783872/.

[49] Ramesh Paudyal et al. “Intravoxel incoherent motion diffusion□weighted MRI during chemoradiation therapy to characterize and monitor treatment response in human papillomavirus head and neck squamous cell carcinoma”. In: *Journal of Magnetic Resonance Imaging* 45.4 (Nov. 2016), pp. 1013–1023. DOI: https://doi.org/10.1002/jmri.25523. URL: https://pubmed.ncbi.nlm.nih.gov/27862553/.

[50] Jerome B Buboltz, Stephen Hendriksen, and Jeffrey S Cooper. *Hyperbaric Soft Tissue Radionecrosis*. July 2023. URL: https://www.ncbi.nlm.nih.gov/books/NBK482261/.

[51] 2024. URL: https://www.cancer.gov/publications/dictionaries/cancer-terms/def/tnm-staging-system.

[52] 2024. URL: https://www.cancer.gov/publications/dictionaries/cancer-terms/def/tnm-staging-system.

[53] Feb. 2018. URL: https://www.cancer.gov/news-events/cancer-currents-blog/2018/microbubbles-radiation-breast-cancer#:~:text=Supplying%20Oxygen%20to%20Boost%20Radiation%20Therapy&text=But%20many%20tumors%20are%20resistant,radicals%2C%20that%20kill%20cancer%20cells..

[54] Joseph R Castro et al. "Carbon Ion Radiotherapy". In: *Elsevier eBooks* (Jan. 2010), pp. 1511–1522. DOI: https://doi.org/10.1016/b978-1-4160-5897-7.00072-x. URL: https://www.sciencedirect.com/topics/nursing-and-health-professions/oxygen-enhancement-ratio#:~:text=The%20oxygen%20enhancement%20ratio%20(OER)%20is%20given%20by%20the%20dose,range%20of%20about%202.5%E2%80%933.0..

[55] X Wang and F.J Hickernell. "Randomized Halton sequences". In: *Mathematical and Computer Modelling* 32.7-8 (Oct. 2000), pp. 887–899. DOI: https://doi.org/10.1016/s0895-7177(00)00178-3. URL: https://scholars.hkbu.edu.hk/en/publications/randomized-halton-sequences.

A. Nomenclature

Abbreviations

Abbreviation	Definition
CR	Complete Response
DWI	Diffusion-Weighted Imaging
HPV	Human Papillomavirus
MRI	Magnetic Resonance Imaging
NG-IVIM	Non-Gaussian Intravoxel Incoherent Motion
OPSCC	Oropharyngeal Squamous Cell Carcinoma
PD	Progressive Disease

Symbols

Symbol	Definition	Unit
ADC	Apparent Diffusion Coefficient	mm^2/s
b	Diffusion Weighting Factor	s/mm^2
D	Diffusion Coefficient	mm^2/s
D^*	Pseudo Diffusion Coefficient	mm^2/s
f	Perfusion Fraction	-
K	Kurtosis	-

B. Fitting model

The fitting model as described in section 2.4 was used to voxel-wise calculate the parameter values. Each parameter was given 1000 initial starting values for each voxel in the GTV according to a Halton sequence [55]. These starting ranges were between $0.24 \cdot 10^{-3}$ and $3.41 \cdot 10^{-3}$ mm^2s^{-1} for ADC and D, $6.29 \cdot 10^{-3}$ and $23.39 \cdot 10^{-3}$ mm^2s^{-1} for D^*, 0.09 and 0.42 for f and 0.1 and 3 for K.

Furthermore, each parameter was also given boundaries to ensure physical plausibility. These ranges were between 0 and $20 \cdot 10^{-3}$ mm^2s^{-1} for ADC and D, 0 and $200 \cdot 10^{-3}$ mm^2s^{-1} for D^*, 0 and 1 for f and 0 and 5 for K. All ranges are based on previous work by Sijtsema et al. [40].

C. Tumor mean parameters changes

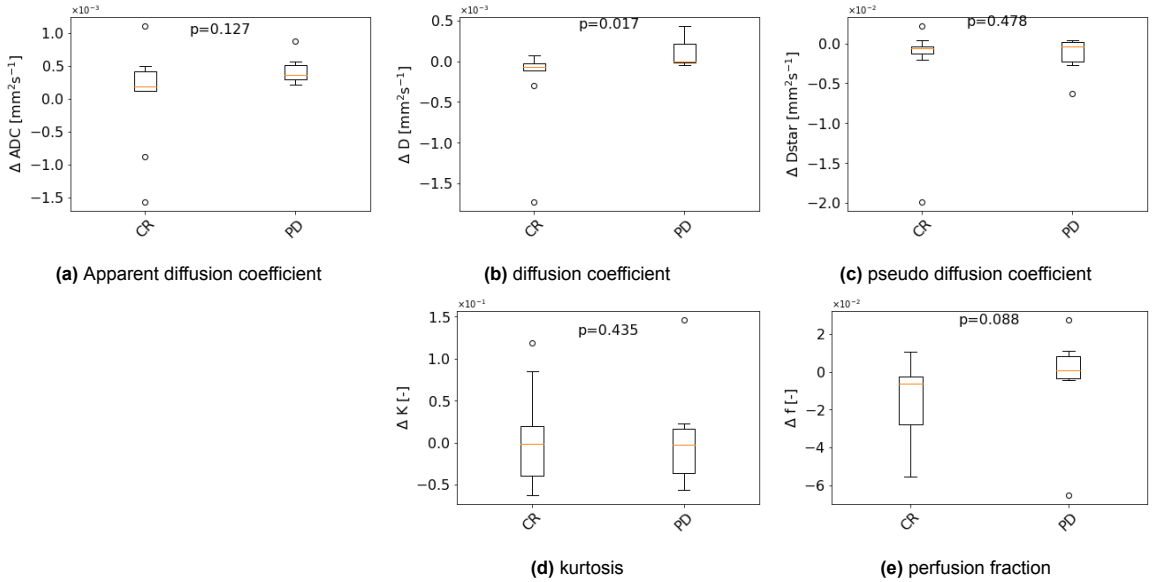

(a) Apparent diffusion coefficient

(b) diffusion coefficient

(c) pseudo diffusion coefficient

(d) kurtosis

(e) perfusion fraction

Figure C.1: Absolute differences between the pretreatment and midtreatment scans divided between Complete response, CR (n = 10) and Progressive disease, PD (n = 6). For the ADC and NG-IVIM parameters.

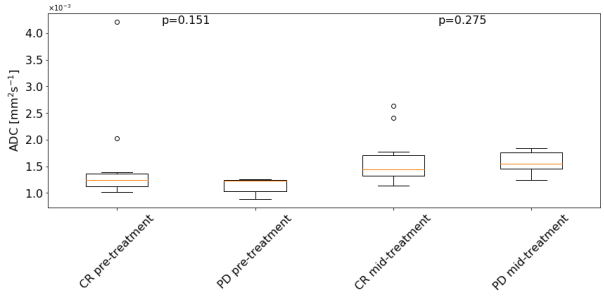

(a) apparent diffusion coefficient

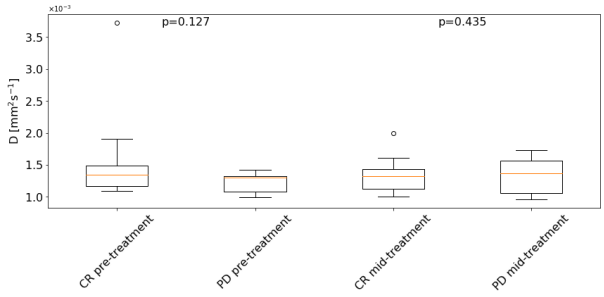

(b) diffusion coefficient

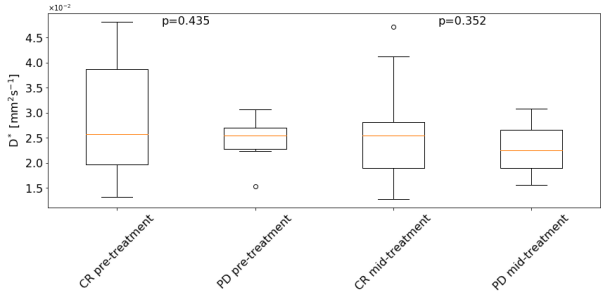

(c) pseudo diffusion coefficient

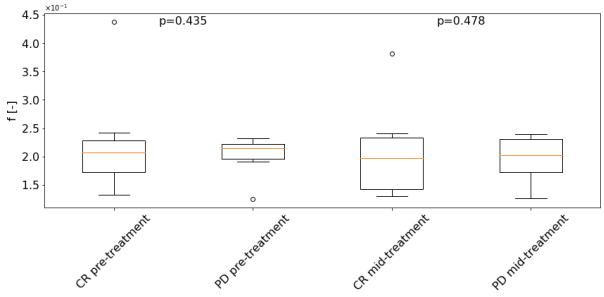

(d) perfusion fraction

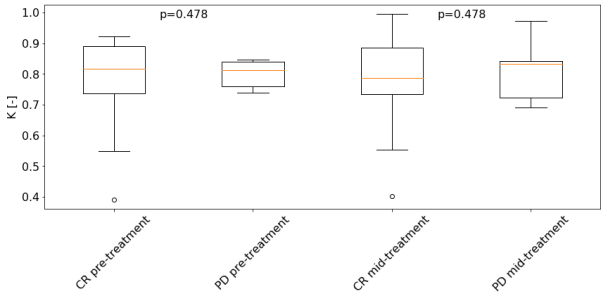

(e) kurtosis

Figure C.2: Tumor mean values for pre- and midtreatment scans splitted between Complete response, CR (n = 10) and Progressive disease, PD (n = 6). For the ADC and NG-IVIM parameters.

D. Tumor heterogeneity

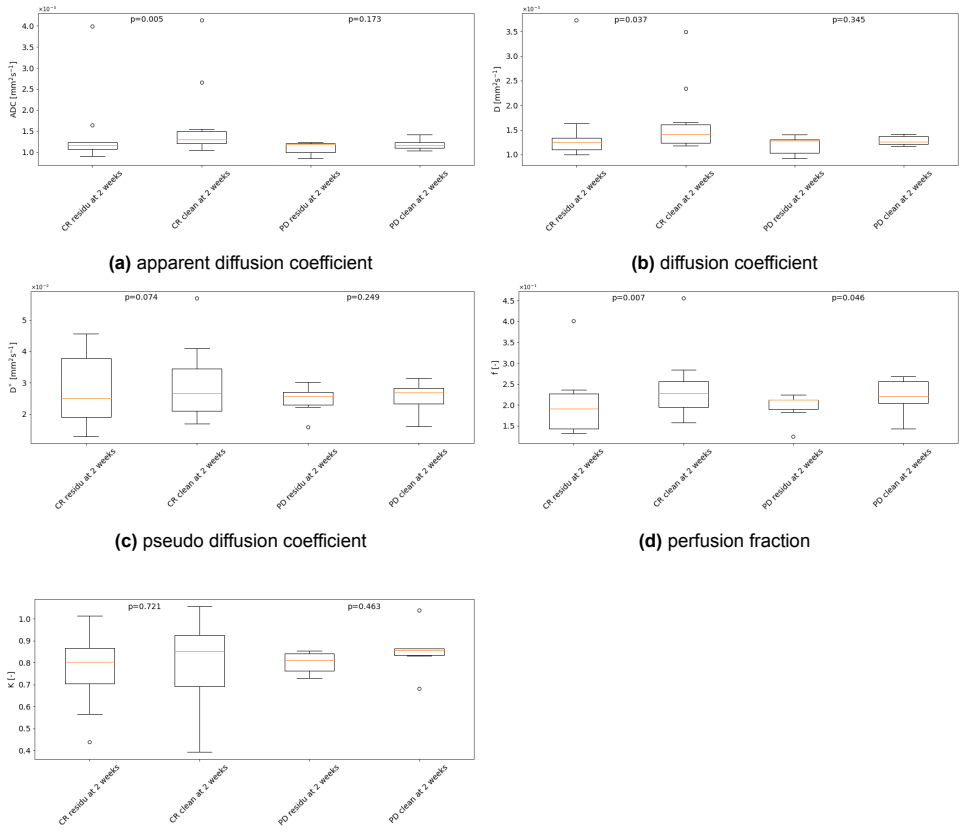

(a) apparent diffusion coefficient

(b) diffusion coefficient

(c) pseudo diffusion coefficient

(d) perfusion fraction

(e) kurtosis

Figure D.1: Mean region results from the regions based on pretreatment scan data, split between Complete response, CR (n = 10) and Progressive disease, PD (n = 6). For the ADC and NG-IVIM parameters.

E. Tumor region shrinkage

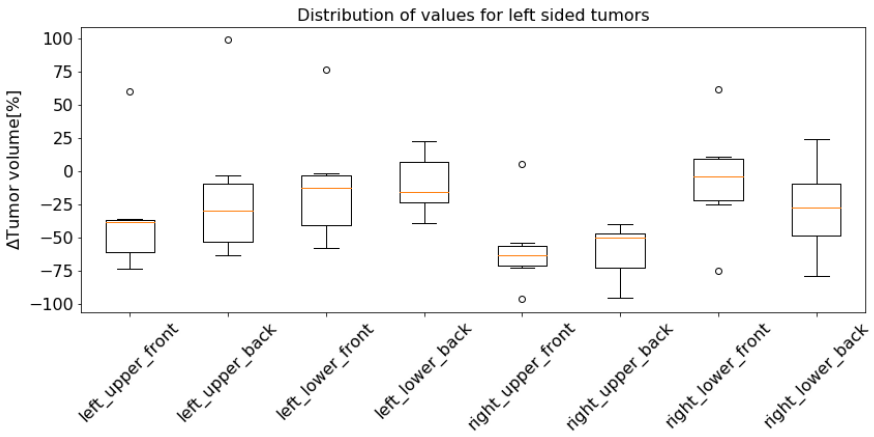

Figure E.1: Tumor decrease for left sided tumor in 8 different regions around the center of volume of the pretreatment GTV

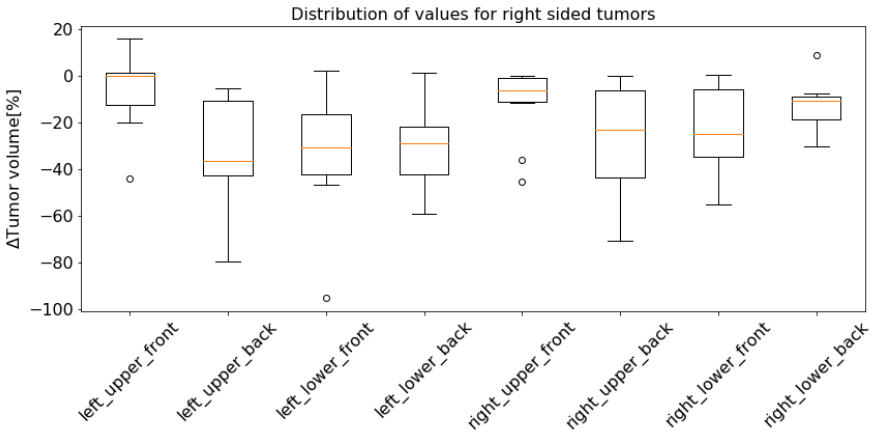

Figure E.2: Tumor decrease for right sided tumor in 8 different regions around the center of volume of the pretreatment GTV